14th International Conference on Structural Safety and Reliability - ICOSSAR'25
1-6 June, 2025 - Los Angeles California, USA
R. Ghanem, E. Johnson, S. Masri and A. Olivier (Eds)

OPTIMAL TIME INTERVALS FOR MAINTENANCE IN JACKET PLATFORMS BASED ON COST-BENEFIT ANALYSIS

GERARDO VARELA[1] AND DANTE TOLENTINO[2]

[1] Departamento de materiales, Universidad Autónoma Metropolitana
420 San Pablo Avenue, Nueva el Rosario, Azcapotzalco, Mexico City 02128, Mexico.
al2211800709@azc.uam.mx

[2] Departamento de materiales, Universidad Autónoma Metropolitana
420 San Pablo Avenue, Nueva el Rosario, Azcapotzalco, Mexico City 02128, Mexico.
dantetl@azc.uam.mx

Key words: Offshore platforms, structural reliability, fatigue damage, cost-benefit analysis, maintenance optimization

Abstract. The development of effective maintenance strategies for offshore platforms is essential to preserve their reliability at acceptable levels. Thus, the environmental and economic consequences of possible structural failures are prevented. This work presents a methodology to estimate the optimal time interval for maintenance actions based on cost benefit analysis (CBA). Structural reliability is estimated in terms of the expected number of failures while the expected total cost considers the cost of inspection, repair and failure in time. Demand exceedance rates are used to estimate demands in time. The uncertainties related to manufacturing process and wave occurrences are considered. The structural damage is defined as the crack growth at different hot spots of the tubular members due to fatigue. Optimal time intervals are estimated on a jacket offshore platform located in the Gulf of Mexico. The results indicate that the optimal time interval is equal to 5 years for systems in which the cost is reduced by about 61% compared to the absence of maintenance. The methodology provides an outline that helps to make the most appropriate decision to extend the useful life of an offshore system.

1 INTRODUCTION

Fixed offshore platforms are a key component of offshore infrastructure, especially in the oil and gas industry. In Mexico, jacket-type platforms managed by Pemex company play a crucial role in hydrocarbon extraction, particularly in the Bay of Campeche. These structures are continuously exposed to environmental and operational loads, which may lead to damage accumulation in time, especially without periodic maintenance where their failure result in significant economic, social, and environmental impacts. Its location in the harsh offshore environment presents unique challenges from design to maintenance and factors such as vessel collisions, earthquakes, corrosion, fatigue, and extreme environmental conditions can compromise safety and production efficiency. Therefore, reliability estimation helps to quantify the structural condition in probabilistic terms and CBA provides informed maintenance planning to ensure structural operability and mitigate progressive deterioration in time. In response to these issues, different strategies have been developed to assess the structural reliability using Monte Carlo simulations to calculate the probability of failure [1], time-dependent capacity degradation models [2], and approaches to estimate the structural reliability considering variations in time of both capacity and demand [3, 4]. In case of CBA, different researchers have improved offshore maintenance planning such as Santa-Cruz and Heredia-Zavoni [5] that propose a decision model considering hydrocarbon prices and maintenance costs to estimate inspection intervals. Tolentino and Ruíz [6] compute the optimal time for maintenance based on CBA. Yoon et al. [7] develop maintenance plans based on structural monitoring and uncertainty. Varela and Tolentino [8] determine optimal intervals using demand exceedance rates and CBA.

Offshore structures need regular inspections and maintenance to preserve their reliability levels in time. With the aim of minimizing possible failures, this study applies CBA to determine the optimal time interval of inspection and repair considering the uncertainties related to material properties and loads. The optimal time interval is estimated on a platform located in the Gulf of Mexico. The structural deterioration is defined by crack growth due to fatigue cracking at critical points in certain joints.

2 STRUCTURAL RELIABILITY IN TIME

The annual expected mean annual failure rate, $E(v_F)$, is as follows [9, 10]:

$$E(v_F) = \int -\frac{dv_D(d)}{dd}\big(P(C \le d)\big)dd \tag{1}$$

where $\frac{dv_D(d)}{dd}$ corresponds to the derivative of the demand hazard function; $P(C \le d)$ represents the probability that the capacity, C, does not exceed a specified performance value, $d.$ To solve Eq. 1, Cornell et al. [11] assume that the hazard curve is as $(y) = ky^{-r}$, where k and r are fitted parameters, and both demand $\widehat{D}$ and capacity $\hat{C}$ follow a lognormal distribution function with variances σ_{UD}^2 and σ_{UC}^2, respectively. Demand is characterized as $\widehat{D} = a \cdot y^b$, with a and b as fitting parameters. The extension to Eq. 1 considering the assumptions of [11] to estimate the mean annual failure rate in time expressed in a closed form expression format is as follows [3]:

$$\bar{\eta}_F(0, \Delta t) = k\left(\frac{\hat{C}(\Delta t)}{a}\right)^{-\frac{r}{b}} e^{\frac{r^2}{2b^2}\left(\sigma_{lnD|h_{max}}^2 + \sigma_{lnC}^2 + \sigma_{UT}^2\right)}\,\Omega(t, \Delta t) \tag{2}$$

where capacity in time is expressed as $\hat{C}(\Delta t) = \alpha_T - \beta_T \Delta t$, and demand for a given wave height, h_{max}, in time is as $\widehat{D}(\Delta t) = (a + f\,\Delta t)\,h_{max}^b$. The total uncertainty σ_{UT}^2 considers the uncertainties of both capacity and demand. The correction factor, $\Omega(t, \Delta t)$, is as follows:

$$\begin{aligned}\Omega(t, \Delta t) = {} & \frac{b\alpha_T}{\beta_T(b-r)}\left(\frac{\alpha_T\beta_T}{-\alpha_T f + \beta_T\alpha_T}\right)^{-\frac{r}{b}}[-F(A;B;C;x) \\ & + F\big(A;B;C;x(\Delta t)\big)\left(1 + \left(\frac{f\beta_T\Delta t}{\beta_T a}\right)^{-\frac{r}{b}}\right)\left(1 + \left(\frac{\beta_T\Delta t}{a}\right)\right)\cdot\left(\frac{\alpha_T + \beta_T\Delta t}{\alpha_T + f\Delta t}\right)^{-\frac{r}{b}}\left(\frac{\alpha_T}{a}\right)^{\frac{r}{b}}]\end{aligned} \tag{3}$$

where $F()$ is a Gaussian hypergeometric function that is solved by means of a hypergeometric series [12].

3 DEMAND EXCEEDANCE RATE

The occurrence of structural demand in time is estimated using the demand exceedance rate, $\upsilon_D(d)$, as follows [11]:

$$\upsilon_D(\lambda_d) = \int_0^\infty v(h_{max}) P(D \geq \lambda_d | h_{max}) dh_{max} \tag{4}$$

where $v(h_{max})$ is the derivative of the wave hazard function; $P(D \geq \lambda_d | h_{max})$ is the wave fragility.

4 COST-BENEFIT ANALYSIS

The CBA proposed by Tolentino and Ruíz [6] estimates the expected total cost by integrating three cost components such as inspection, repair, and failure. Then, the total cost, $\bar{C}_{TOT}(0, \Delta t)$, is defined as the sum of inspection $\bar{C}_{INS}(0, \Delta t)$, repair, $\bar{C}_{REP}(0, \Delta t)$, and failure cost, $\bar{C}_{FAI}(0, \Delta t)$ as follows:

$$\bar{C}_{TOT}(0, \Delta t) = \bar{C}_{INS}(0, \Delta t) + \bar{C}_{REP}(0, \Delta t) + \bar{C}_{FAI}(0, \Delta t) \tag{5}$$

where:

$$\bar{C}_{INS}(0, \Delta t) = \sum_{m=1}^{NI} C_{I_m | q, \Delta t} e^{-\gamma_m(\Delta t) - \bar{\eta}_F(0, \Delta t)} \tag{6}$$

$$\bar{C}_{REP}(0, \Delta t) = \sum_{m=1}^{NI} \sum_{j=1}^{n} C_{R_j | q, \Delta t} P\left(D_{j,m}(\Delta t) \geq d\right) e^{-\gamma_m(\Delta t) - \bar{\eta}_F(0, \Delta t)} \tag{7}$$

$$\bar{C}_{FAI}(0, \Delta t) = \sum_{m=1}^{NI} C_{F_m | DI, \Delta t} \sum_{k=1}^{\hat{N}} \bar{\eta}_F(t_k - t_{k-1}) e^{-\gamma_m(\Delta t) - \bar{\eta}_F(0, t_k - t_{k-1})} \tag{8}$$

where the inspection cost considers the costs associated with scheduled inspections during a given time interval, $C_{I_m | q, \Delta t}$, for a given quality of inspection, q. The repair cost, $C_{R_j | q, \Delta t}$, considers the cost associated to repair of the $j-th$ element at Δt for a given a specific q; n is the number of critical joints for repair. The failure cost, $C_{F_m | DI, \Delta t}$, is estimated based on global damage index, DI, at Δt; $\gamma_m(\Delta t)$ is the discount rate; $\hat{N}$ corresponds to the number of intervals considered and $NI = \frac{DL}{\Delta t}$ represents the number of inspections that must be completed during a time interval, DL.

The quality of an inspection, q, is influenced by factors such as the inspection technique, size of the crack, and the equipment used. The probability of detecting a crack of a certain size, $PoD(x)$, is directly linked to inspection quality and can be modeled using logistic, lognormal, or exponential distributions [13]. In this study, $PoD(x)$ is estimated using the following expression [14]:

$$PoD(x) = 1 - exp\left(\frac{x - a_{min}}{\lambda}\right), \quad a > a_{min} \tag{9}$$

where a_{min} is equal to 2 mm [15], and λ is estimated as $\lambda = \frac{1}{q}$, where q takes values between 0.2 and 0.3 [6].

5 ILLUSTRATIVE EXAMPLE

The optimal time interval based on the CBA is estimated on a steel jacket offshore platform located at the Och site in the Bay of Campeche. The structure has a height of 72.58 meters and is found in water depths of 60 meters (see Figure 1). The structural system has tubular steel elements with different diameters and thicknesses (see Table 1). The piles within the platform legs are designed to transmit vertical, horizontal, and bending loads.

Table 1: Geometric properties

Elements	*D* (m)	*T* (m)
05, 18 and 27	0.508	0.0191
17, 19, 21, 22, 26, 28, 30, 31, 32 and 33	0.610	0.0191
35, 36, 38, 39, 40 and 41	0.610	0.0254
23 and 24	0.660	0.0159
08, 09, 14 and 15	0.762	0.0159
01 and 02	0.762	0.0191
04, 06, 11 and 12	0.762	0.0254
03, 07, 10, 13, 16, 20, 25 and 29	1.460	0.0191
34 and 37	1.500	0.0413

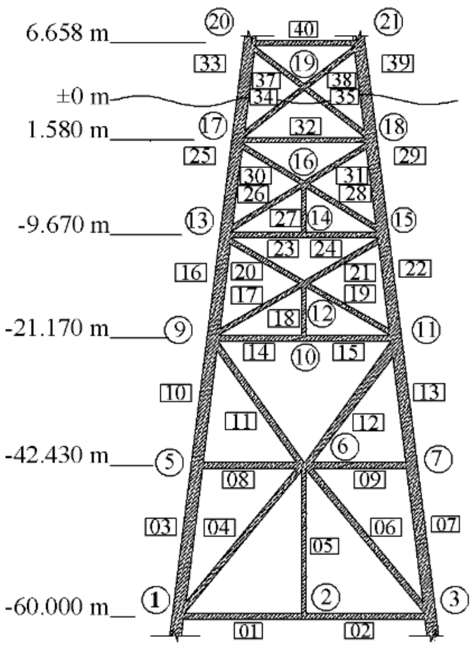

Figure 1: Offshore system

5.1 Expected properties of materials and loads for offshore platforms

The study considers the uncertainties related to materials such as steel grades ASTM A36, ASTM A572 Grade 50 and modulus of elasticity as well as the uncertainties associated to dead load. Table 2 shows the statistics of both material properties and load used in this study.

Table 2. Statistical properties of materials and load

Property	Distribution type	Mean (μ)	Standard deviation (σ)	Reference
Yield stress (ASTM A36)	Log-normal	0.1903	0.0989	[16]
Yield stress (ASTM A572 Gr. 50)	Log-normal	0.1746	0.1214	[16]
Elastic modulus (E)	Log-normal	-0.013525	0.0752	[16]
Dead load	Normal	1	0.0011	[17]

5.2 Environmental hazard

The PEMEX code [18] provides detailed information on the environmental loads that affects the region. Figure 2 shows the environmental hazard curves for the site.

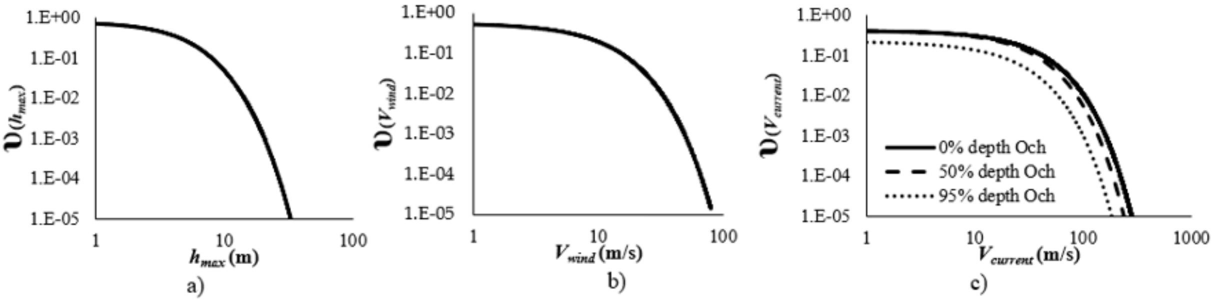

Figure 2: Hazard curves of a) wave, b) wind speed and c) sea current speed.

5.3 Fatigue analysis

Offshore structures are exposed to environmental loads that can degrade in time their mechanical properties. Critical joints, identified as those with the greatest influence on the overall capacity of the structure, are selected by non-linear static analyses. In this process, the capacity of one joint is reduced, then, the response of the system is calculated by means of pushover analysis. If the joint reduction contributes significantly to structural behavior, it is classified as critical joint. The above process is repeated for each joint in the system. For the platform under study, the critical joints are 1-7, 9-11, and 13. Each end of the tubular element that is part of a critical joint is assumed to contain two hot spots. On the other hand, the sea state is considered fully developed that allows the waves to model as a homogeneous Gaussian stationary process. Then, the Pierson-Moskowitz spectrum [19] is used to characterize wave frequency content. The crack size at each hot spot is calculated using Monte Carlo technique considering thirty thousand simulations. It is assumed that the time intervals between storms follow an exponential distribution [20]. Crack propagation is a complex process because it is not constant over time. Paris introduced the concept of the average stress intensity interval, ΔK_{mr}, to characterize crack growth per cycle, da/dN [21, 22]. The crack size assessment at the hot spots under random loading is estimated using Paris law and the random fatigue theory of Sobczyk and Spencer [23] as follows:

$$\frac{da'}{dt} = C(\Delta K_{mr})^m v' \ , \ \Delta K_{mr} = Y S_{mr}\sqrt{\pi a'} \qquad (10)\ (11)$$

where C and m are Paris constants; ΔK_{mr} represents the mean value of the stress intensity interval; ν' is the positive zero-crossing rate; Y is a geometric correction factor [24]; S_{mr} is the mean value of the stress interval for each element [23], and a' is the crack size. Substituting Eq. 11 into Eq. 12 and performing algebraic steps leads to the following expression:

$$\int_{a_0}^{a_f} \frac{da}{\left(Y\sqrt{\pi a'}\right)^m} = CS_{mr}^m v' t \tag{12}$$

where a_0 is the initial crack size, and a_f is the crack size at the end of N cycles. The Paris constants are defined by the research of Silva-González and Heredia-Zavoni [1], who defined statistical parameters for offshore systems in Campeche Bay (see Table 3). [25] propose the reduction of joint capacity due to fatigue, P_c, as $P_c = P_k\left(1 - A_{crack}/A_{join}\right)$, where P_k represents the joint's capacity without damage, A_{crack} is the damaged area of the elements connected to the joint, and A_{join} is the original joint area. Figure 3 shows the capacity reduction at different time instants for joints 5 and 9 of the Och platform.

Table 3. Statistical parameters for crack simulations [1].

Parameter	Distribution	Mean	Standard deviation
V_0	Lognormal	Changes for each joint in time	Changes for each joint in time
S_{mr}	Rayleigh	Changes for each joint in time	Changes for each joint in time
$M*$	Normal	3	0.3
$InC*$	Normal	-40.39	-0.69067
a/c	-	0.25	-
a_0	-	0.00011	-

* Correlation coefficient, ρ, equal to 0.9

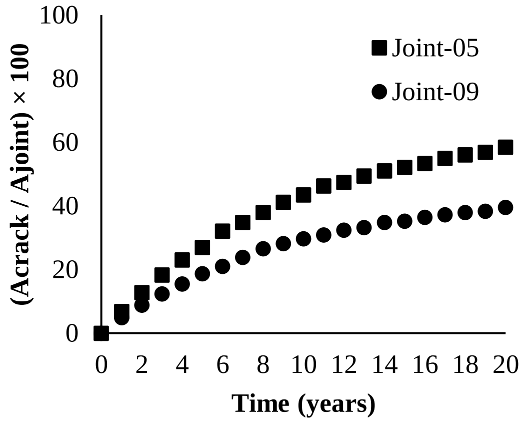

Figure 3: Joint capacity reduction in time.

5.4 Structural capacity and demand

The structural capacity was evaluated through nonlinear static analyses using 50 load profiles that represent the effects of maximum waves of the region. The above loads are associated with 128 offshore systems with uncertain properties, then 6400 nonlinear static analyses are performed. The structural deterioration is modeled by the reduction of the capacity of each critical joint due to fatigue (see Section 5.3). Figure 4 shows the evolution of structural capacity in time and plus/minus one standard deviation. The structural capacity in time of each system simulation is fitted as $\hat{C}_i(t) = \alpha_i + \beta_i t$, where α_i and β_i are parameters that fitted the linear regression. It is noticed that the structural capacity of the systems decreases in time and, as time passes, the variability of the responses increases, leading to a higher value of the standard deviation

The structural demand in time was estimated through incremental nonlinear dynamic analyses using 50 load profiles associated with 5 return periods in accordance with PEMEX code [43]. The crack growth used to estimate the capacity in time is implemented to compute the demand in time. The 128 systems with uncertain proprieties are used in this section, then, 32000 nonlinear dynamic analyses were performed. Figure 5 illustrates the surface of the mean structural demand and a shaded band that represents plus/minus one standard deviation. For each simulated structure, the demand was fitted according to the expression $\widehat{D}_i(t) = (a_i + f_i t) {h_{max}}^{b_i}$, where a_i, f_i, and b_i are the fitted parameters for the $i-th$ simulation. The structural demand in time exhibits an increase of 116% over 20 years. Demand remains constant for wave heights below 16.7 m that indicates linear elastic behavior. Results highlight the increasing trend of structural demand in time.

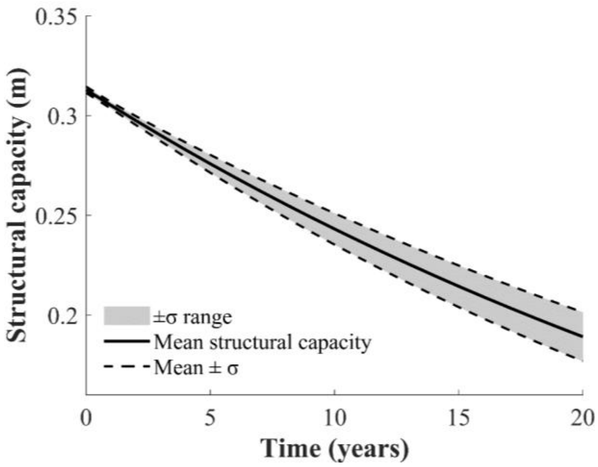

Figure 4: Structural capacity in time.

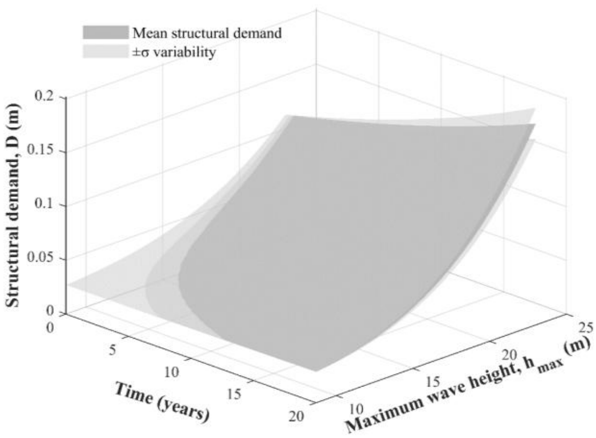

Figure 5: Structural demand in time.

5.6 Demand exceedance rate

The demand exceedance rate indicates the number of times that structural demand is exceeded per unit of time. The numerical results given by Eq. 4 can be characterized by the following expression [26]:

$$v_D(d) = \left(\frac{\lambda_d}{\lambda_{d_0}}\right)^{-\varphi} \left(\frac{\lambda_{d_{max}} - \lambda_d}{\lambda_{d_{max}} - \lambda_{d_0}}\right)^{\varepsilon} \quad (13)$$

where λ_{d_0} is the minimum demand value, $\lambda_{d_{max}}$ is the maximum demand value, and φ and ε are fitting parameters. Each simulated structure presents individual values of the parameters indicated in Eq. 4. Demand exceedance rates for each simulated structure are estimated in terms of maximum global displacement for λ_d values between 0.01 to 0.23 m. An example of one simulated system is shown in figure 6 where the exceedance rate is 0.4008 for 0.025 m, corresponding to a return period of 2.49 years. Under the design condition (maximum wave height $h_{max} = 16.7$ m), the exceedance rate is λ_d =0.075 m with a return period of 7.02 years. For the ultimate condition ($h_{max} = 23$) $\lambda_d = 0.106$ at $\Delta t = 0$ has an exceedance rate of 0.0213, resulting in a return period of 46.94 years. Demand simulations are performed via the inverse transformation method. The cumulative distribution function is expressed as:

$$F(y) = 1 - v_D(d)/v_0 \quad (14)$$

where v_0 represents the exceedance rate associated with the λ_{d_0} considered. The structural demand occurrence is determined using the expression $T_{\mathrm{i}} = -\left|\frac{\ln(u)}{v^0}\right|$ [27], where u denotes random numbers. Subsequently, 2000 realizations of structural demand and waiting times are generated for each simulated structure. Figure 7 shows an example of one such realization.

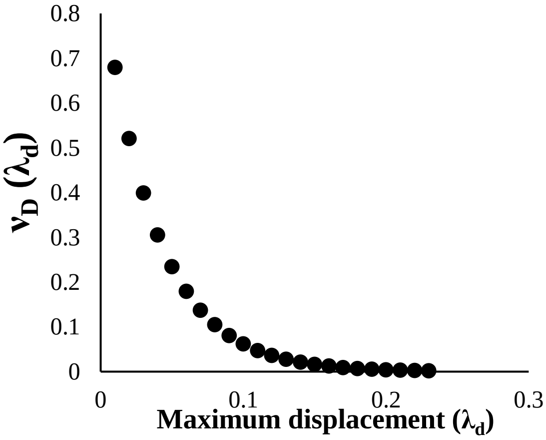

Figure 6: Numerical demand exceedance rates**.**

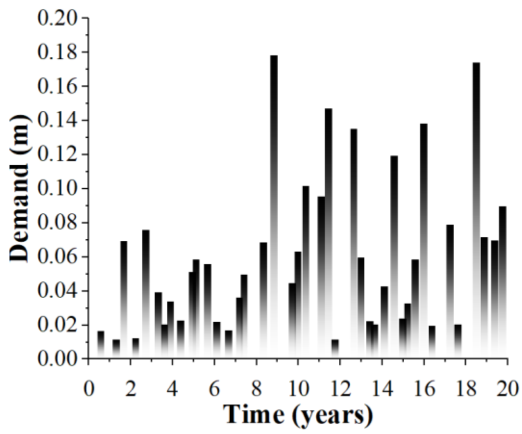

Figure 7: Demand and waiting times.

5.7 Optimal inspection interval

The optimal time interval is determined by analyzing 2000 realizations per simulated structure, considering structural demand, waiting times, and costs associated with inspection, repair, and failure. The inspection cost per joint is equal to 3518 USD [28], and repair costs are applied when the probability of a crack exceeding 4 mm is exceeding [29]. The cost of repair each joint is equal to 20,000 USD [30]. Failure costs $C_{F_{m,i}|DI_i,\Delta t}$ are calculated based on structural damage expressed in terms of the normalized damage index, DI_i, as follows [31]:

$$DI_i = \frac{C_{0,i} - C_i(\Delta t)}{C_{0,i} - D_i(\Delta t)} \quad (15)$$

where C_0 is the initial structural capacity, and (Δt) and $D(\Delta t)$ are the capacity and demand at time Δt, respectively. Indirect losses are estimated as:

$$C_{PID} = C_{F_T}\left(\frac{P_m}{P_t}\right) DI_i^4 \quad (16)$$

where C_{F_T}= 1.086× 10^{10} USD, $Pm = 184{,}000$/day, and the total daily oil extraction, P_t in Campeche Bay is 2,100,000 barrels. Pollution costs are calculated as:

$$C_{POD} = \frac{C_{OR} S_A E_f}{1 \times 10^6} \quad (17)$$

where C_{OR}=541.57 USD/hr, $Ef = 8.1 \times 10^{-1}$ h/km², and the affected area S_A is:

$$S_A = 4 \times 10^{-2} \Delta w P_m DI^4 U^4 + 2.27 \sqrt[3]{(\Delta w P_m DI_i^4)^2}\sqrt{t} \quad (18)$$

where Δw is equal to 6.341 × 10^{-2} (density difference between water and oil), $t = 2400$ seconds, and U is 30m/s. Deferred production costs $C_{DPC}$are computed as:

$$C_{DPC} = 365 \int_t^L C_C P_m U_C \exp[-\gamma(\tau - t)] d\tau - 365 \int_t^{L+T_{RP}} C_C P_m U_C \exp[-\gamma(\tau - t)] d\tau \quad (19)$$

where $L = 30$ years [6], C_C = 92 USD/barrel [32], U_C = 12% (sales gain), T_{RP}= 4 years [33], and $\gamma = 3.13\%$ (discount rate). Equipment damage costs, C_{EQD}, are directly proportional to the structural damage and are calculated as $DI_i \cdot C_{EQPT}$, where C_{EQPT} is the drilling equipment cost, valued at 130,000,000 USD [34].

The expected total cost is influenced by demand, capacity, and crack size, simulated using lognormal distributions for crack size $a(t)$ and fitting parameters from Table 3. Figure 8 shows the expected costs, the dispersion is associated with uncertainties related to material, loads, crack growth due to fatigue analysis and structural responses. It is observed that short inspection intervals result with higher variability for inspection and repair costs, while longer intervals exhibit a greater dispersion for failure costs. This variability is explained by inspection quality that is influenced by crack detection between 1-3 years and maintenance actions that are activated after four years. Inspection and repair costs tend to decrease as the inspection interval increases while failure costs increase, especially after the 5-year interval. The dispersion observed in Figure 8 highlights the variability induced by uncertain properties. The results show that the optimal time interval for maintenance actions is equal to 5 years.

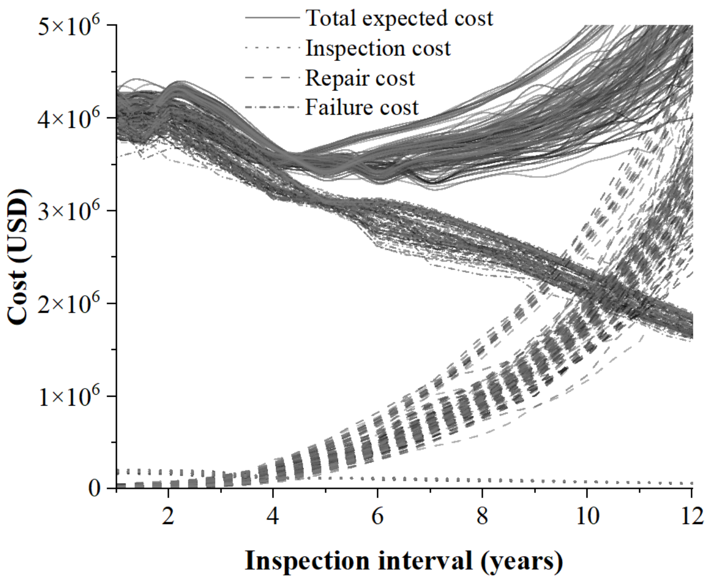

Figure 8: Expected cost considering all simulated

6 CONCLUSIONS

The optimal time interval for maintenance activities based on CBA is estimated. The optimal time interval considers the inspection, repair, and failure costs. The costs involve the structural reliability expressed through the expected number of failures. The concept of demand exceedance rate is used to estimate the expected costs of failure. The methodology used is versatile and can be adapted to different environmental conditions and structural systems and it is not limited to offshore structures.

The results indicate that the optimal interval for maintenance actions is equal to 5 years which represents a balance between cost and an acceptable reliability level. These results are important for the management and planning of structural maintenance. However, the optimal time interval could change if another phenomenon, such as corrosion, is considered. The work has two limitations, the first is related to the estimation of hypergeometric functions and the second is associated with a high demand for computational calculation. Future research could focus on comparing this methodology with alternative approaches, such as multi-objective optimization. Moreover, the expression to estimate the expected number of failures in time can be improved by proposing enhancements to the hypotheses made for its derivation.

ACKNOWLEDGEMENTS

The first author thanks SECIHTI for financial support, and both authors thank Universidad Autónoma Metropolitana for institutional support.

REFERENCES

[1] Silva-González, F.L., and Heredia-Zavoni, E., Effect of uncertainties on the reliability of fatigue damaged systems. (2004) **2**:427–434.

[2] Torres, M.A., and Ruíz, S.E., Structural reliability evaluation considering capacity degradation over time. *Eng. Struct.* (2007) **29**:2183–2192.

[3] Tolentino, D., Ruiz, S.E., and Torres, M.A., Simplified closed-form expressions for the mean failure rate of structures considering structural deterioration. *Struct. Infrastruct. Eng.* (2012) **8**:483–496.

[4] Tolentino, D., and Ruíz, S.E., Time-dependent confidence factor for structures with cumulative damage. *Earthq. Spectra* (2015) **31**:441–461.

[5] Santa-Cruz, S., and Heredia-Zavoni, E., Maintenance and decommissioning real options models for life-cycle cost-benefit analysis of offshore platforms. *Struct. Infrastruct. Eng.* (2009) **7**:733–745.

[6] Tolentino, D., and Ruiz, S.E., Influence of structural deterioration over time on the optimal time interval for inspection and maintenance of structures. *Eng. Struct.* (2014) **61**:22–30.

[7] Yoon, J.T., Youn, B.D., Yoo, M., Kim, Y., et al., Life-cycle maintenance cost analysis framework considering time-dependent false and missed alarms for fault diagnosis. *Reliab. Eng. Syst. Saf.* (2019) **184**:181–192.

[8] Varela, G., and Tolentino, D., Cost–benefit assessment of offshore structures considering structural deterioration. *J. Mar. Sci. Eng.* (2023) **11**:1348.

[9] Cornell, C.A., Engineering seismic risk analysis. *Bull. Seismol. Soc. Am.* (1968) **58**:1583–1606.

[10] Esteva, L., Bases para la formulación de decisiones de diseño sísmico, Instituto de Ingeniería, Universidad Nacional Autónoma de México, (1968). (in Spanish)

[11] Cornell, C.A., Jalayer, F., Hamburger, R.O., and Foutch, D.A., Probabilistic basis for 2000 SAC federal emergency management agency steel moment frame guidelines. *J. Struct. Eng.* (2002) **128**:526–533.

[12] Rainville, D., Intermediate course in differential equations, Wiley, (1961).

[13] Visser, W., POD/POS curves for non-destructive examination. (2002).

[14] Rangel-Ramirez, J.G., and Sørensen, J.D., Optimal risk-based inspection planning for offshore wind turbines. *Int. J. Steel Struct.* (2008) **8**:295–303.

[15] Moan, T., Reliability-based management of inspection, maintenance and repair of offshore structures. *Struct. Infrastruct. Eng.* (2007) **1**:33–62.

[16] Hess, P.E., Bruchman, D., Assakkaf, I.A., and Ayyub, B.M., Uncertainties in material and geometric strength and load variables. *Nav. Eng. J.* (2002) **114**:139–166.

[17] Fjeld, S., Reliability of offshore structures. *J. Pet. Technol.* (1978) **30**:1486–1496.

[18] PEMEX, Diseño y evaluación de plataformas marinas fijas en la sonda de Campeche, (2000). (in Spanish)

[19] Pierson, W.J., and Moskowitz, L., A proposed spectral form for fully developed wind seas based on the similarity theory of S. A. Kitaigorodskii. *J. Geophys. Res.* (1964) **69**:5181–5190.

[20] Lee, S., Wilson, J.R., and Crawford, M.M., Modeling and simulation of a nonhomogeneous poisson process having cyclic behavior. *Model. Simul. a Nonhomogeneous Poisson Process Having Cycl. Behav.* (2007) **20**:777–809.

[21] Paul Paris, Mario P. Gómez, and William E. Anderson, A rational analytic theory of

fatigue. *Trend Eng.* (1961) **13**:9.
[22] Paris, P., and Erdogan, F., A critical analysis of crack propagation laws. *J. Basic Eng.* (1963) **85**:528–533.
[23] Sobczyk, K., Spencer, B.F., and Jr., B.F.S., Random fatigue: From data to theory, Academic Press, (1992).
[24] Newman, J.C., and Raju, I.S., An empirical stress-intensity factor equation for the surface crack. *Eng. Fract. Mech.* (1981) **15**:185–192.
[25] Stacey, A., Sharp, J. V, and Nichols, N.W., Static strength assessment of cracked tubular joints, (1996).
[26] Tolentino, D., Flores, R.B., and Alamilla, J.L., Probabilistic assessment of structures considering the effect of cumulative damage under seismic sequences. *Bull. Earthq. Eng.* (2018) **16**:2119–2132.
[27] Tolentino, D., Márquez-Domínguez, S., Gaxiola-Camacho, R., Márquez-Domínguez, S., et al., Fragility assessment of bridges considering cumulative damage caused by seismic loading. *KSCE J. Civ. Eng.* (2020) **24**:1–10.
[28] Raine, A., The development of alternating current field measurement (ACFM) technology as a technique for the detection of surface breaking defects in conducting material and its use in commercial and industrial applications, in: *Proceedings of the 15th World Conference on Non-Destructive Testing*, (2000).
[29] Kirkemo, F., Applications of probabilistic fracture mechanics to offshore structures. *Appl. Mech. Rev.* (1988) **41**:61–84.
[30] MTD, T.M.T.D.L., New design methods for offshore piles. *Publ. 94/102* (1994).
[31] Tolentino, D., and Ruíz, S.E., Time intervals for maintenance of offshore structures based on multiobjective optimization. *Math. Probl. Eng.* (2013) **2013**:1–15.
[32] BANXICO, Precio de la mezcla mexicana de petroleo. (2023). (in Spanish)
[33] Estrada, C.E.O., and De León Escobedo, D., Development of a cost-benefit model for inspection of offshore jacket structures in Mexico, in: *Proceedings of the International Conference on Offshore Mechanics and Arctic Engineering - OMAE*, (2003), pp. 87–98.
[34] IMP, Resumen ejecutivo de costos promedio de estructuras típicas ubicadas en la sonda de Campeche, (1998). (in Spanish)